

Lattice versus continuum theory of the periodic Heisenberg chain

Michael Bortz,^{1,*} Michael Karbach,² Imke Schneider,¹ and Sebastian Eggert¹

¹*Fachbereich Physik, Technische Universität Kaiserslautern, Erwin-Schrödinger-Str., D-67663 Kaiserslautern, Germany*

²*Fachbereich Mathematik und Naturwissenschaften, Physik, Bergische Universität Wuppertal, D-42097 Wuppertal, Germany*

(Received 1 April 2009; revised manuscript received 15 May 2009; published 11 June 2009)

We consider the detailed structure of low-energy excitations in the periodic spin-1/2 XXZ Heisenberg chain. By performing a perturbative calculation of the nonlinear corrections to the Gaussian model obtained from bosonization, we determine the exact coefficients of asymptotic expansions in inverse powers of the system length N for a large number of low-lying excited energy levels. This allows us to calculate eigenenergies of the lattice model up to order $\mathcal{O}(N^{-4})$, without having to solve the Bethe ansatz equations. At the same time, it is possible to express the exact eigenstates of the lattice model in terms of bosonic modes.

DOI: 10.1103/PhysRevB.79.245414

PACS number(s): 75.10.Pq, 05.30.-d, 02.30.Ik

I. INTRODUCTION

Quantum models defined on discrete lattices are very common in solid-state theory. Two routes to study their properties are conceivable: either the attempt to solve the model on the lattice, or the formulation of an effective-field theory in the continuum. Lattice models are much more tractable than continuum theories in numerical simulations. On the other hand, within the field-theoretical picture, it is often possible to describe the spectrum in terms of noninteracting or weakly interacting quasiparticles, which makes this approach very attractive from an analytical point of view. Thus, it is most desirable to express the lattice eigenstates in terms of the conceptually much simpler field-theoretical eigenstates.

This goal is generally not achievable since neither the lattice model nor the full field theory can be solved without approximations. Integrable one-dimensional models, however, are the most promising candidates where such a description can be realized quantitatively. Indeed, the effective bosonic theory of the spin-1/2 XXZ Heisenberg chain offers the opportunity to obtain the lattice eigenenergies as an asymptotic expansion in the inverse system length, and at the same time to express the exact lattice eigenstates as linear combinations of bosons. So far, finite-size corrections to the bosonic spectrum have been determined quantitatively for particle excited states.^{1,2} We now calculate the coefficients of the asymptotic corrections quantitatively for current and particle-hole excited states as well.

In particular, we obtain the leading terms in an expansion of the lattice energies in the inverse system length to order $\mathcal{O}(N^{-4})$, which translates into a relative deviation of a fraction of a percent or less already for moderate chain lengths $N \sim 20-100$. This is achieved for a large number of low-lying levels, including those for which exact Bethe ansatz (BA) data are difficult to obtain due to strings of the BA quasimomenta in the complex plane. Furthermore, we express the lattice eigenstates in terms of their bosonic counterparts. Since these states are then eigenstates of a free bosonic theory, our results have the potential to calculate expectation values of local operators in excited states.

We consider the Hamiltonian of the XXZ model

$$H = \sum_{j=1}^N (S_j^x S_{j+1}^x + S_j^y S_{j+1}^y + \Delta S_j^z S_{j+1}^z), \quad (1)$$

with periodic boundary conditions and N lattice sites. We restrict ourselves here to the critical regime $-1 < \Delta < 1$; data for the isotropic point $\Delta=1$ are given in Appendix A.

By a Jordan-Wigner transformation, Eq. (1) can be mapped to a model for itinerant spinless fermions. The corresponding Hamiltonian reads

$$H_f = \frac{1}{2} \sum_{j=1}^N \left[c_j^\dagger c_{j+1} + c_{j+1}^\dagger c_j + 2\Delta \left(n_j - \frac{1}{2} \right) \left(n_{j+1} - \frac{1}{2} \right) \right] - \frac{1}{2} (1 + e^{i\pi M}) (c_N^\dagger c_1 + c_1^\dagger c_N), \quad (2)$$

where $n_j = c_j^\dagger c_j$ and M is the total number of particles, i.e., the eigenvalue of the total number operator $\sum_{j=1}^N n_j$, which commutes with H_f . Thus for an odd (even) number of particles, the boundary conditions of Eq. (2) are cyclic (anticyclic). The models in Eqs. (1) and (2) have significant experimental relevance, either in crystals with a strongly anisotropic spin exchange^{3,4} or in quasi-one-dimensional itinerant electron models such as carbon nanotubes.⁵⁻⁷ Most recently, central quantities such as the dynamical structure factor⁸ and the local density of states⁹ have been calculated for the lattice model (1) from sums over contributions of individual states.

Historically, the model (1) has been studied extensively as a prototypical interacting many-body quantum system. The exact solution for $\Delta=-1$ was found by Bethe;¹⁰ Hulthen described the isotropic antiferromagnet $\Delta=1$.¹¹ This solution was generalized to arbitrary Δ by des Cloizeaux and Gaudin.¹² From these works, the ground state and the ground-state energy were derived by Yang and Yang.¹³ Excitations above the ground state were constructed by Takahashi (for a review, see Ref. 14).

Whereas those works rely on the exact solution of the lattice model, a field-theoretical approach revealed that excitations with an energy $\Delta E = \mathcal{O}(1/N)$ above the ground state can be described asymptotically, which is in the limit of large chain lengths, in terms of free quasiparticles that obey bosonic statistics (for a review, see Ref. 15). The corresponding effective Hamiltonian is the Gaussian model, which leads

to degeneracies between certain bosonic excitations. Interactions between quasiparticles are captured in additional irrelevant operators,¹ which yield nonlinear contributions to the spectrum and generally lift the degeneracies.

Conformal invariance relates the finite-size scaling behavior of each eigenenergy to the scaling dimensions of the operators in the effective-field-theoretical model.^{16–18} This connection has been used to predict the scaling dimensions of the leading irrelevant operators.^{19,20} Here, we employ finite-size scaling to demonstrate the lifting of degeneracies for individual levels by calculating the exact contribution of the irrelevant operators to lowest order.

Therefore, we first concentrate on those low-lying excitation levels that can be computed numerically from the BA for arbitrary N without convergence problems. These are mostly parametrized by real BA quasimomenta. After having done this check, we can use our method to calculate low excitation energies of the lattice model with an accuracy of $\mathcal{O}(N^{-4})$ for $\Delta < 1/2$, and $\mathcal{O}(N^{-2K})$, $K = \pi/(\pi - \arccos \Delta)$ for $1/2 < \Delta < 1$, without using the BA equations, regardless of the underlying BA quasimomenta distribution. Thus especially for $\Delta < 1/2$, we obtain very accurate analytic results for low-lying excitation energies even of relatively short chains without having to deal with the BA equations at all, thus also avoiding string solutions.

Using this procedure, we then tackle the so far unanswered question of how lattice eigenstates are expressed in terms of bosonic states. This will help in constructing the “physical” excitations seen in *ab initio* numerical methods or experiments as linear combinations of bosons.⁹

The remainder of this paper is organized as follows: Sec. II starts with a pedagogical introduction into the $\Delta=0$ model and then treats the BA solution for general Δ . In the third section, the effective low-energy solution from bosonization is presented, including leading and higher-order contributions. The lattice eigenstates and eigenenergies are expressed asymptotically through the eigenstates and eigenenergies of the bosonic low-energy effective Hamiltonian. The relative error in this asymptotic expansion is illustrated in Sec. IV from a numerical finite-size analysis. Appendix A illustrates the conformal towers at the special points $\Delta=0, 1/2, 1$, and Appendix B contains a table (Table I) that illustrates our labeling of the BA levels for $N=8$.

II. EXACT LATTICE SOLUTION

This section summarizes the exact solution of the lattice model. In order to introduce our labeling of the energy levels in the large- N limit, we start with a pedagogical introduction into the noninteracting case $\Delta=0$. The BA solution is presented afterward.

A. Free model

After a Fourier transformation of Eq. (2), the energy levels for the free model are given by

$$E(\{k_j\}) = - \sum_{j=1}^M \cos k_j, \quad S^z = \frac{N}{2} - M, \quad (3)$$

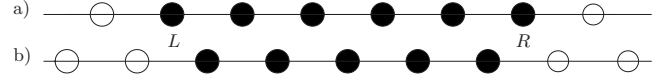


FIG. 1. (a) Sketch of the ground state and (b) of a spin excitation $S^z=1$, where one phase is removed and the remaining ones are again grouped symmetrically without vacancies. Here, (a) the ground state is composed of an even number of particles while (b) the excited state consists of an odd particle number.

$$k_j = \frac{2\pi n_j}{N}, \quad (4)$$

where the M -many phases n_j are chosen out of the N possible values $-(N+1)/2 + p$, $p=1, \dots, N$. We denote the values which are not occupied by a phase as “vacancies.” Here, we restrict ourselves to even N , where $S^z=0, 1, \dots, N/2$. The lowest state in each S^z sector (or equivalently, with M -many particles) is given by the dense and symmetric distribution of the phases, without any vacancies, see Fig. 1(a). This means that the n_j in Eq. (4) are integer (half-integer) for M odd (even), corresponding to cyclic (anticyclic) boundary conditions in Eq. (2). The ground-state energy E_0 has no net magnetization, i.e., $M=N/2$, and its leading terms in a large- N expansion are then given by

$$E_0 = - \sum_{j=0}^{N/2-1} \cos \frac{\pi}{N} \left(2j - \frac{N}{2} + 1 \right) \\ = - \frac{1}{\sin(\pi/N)} = - \frac{N}{\pi} - \frac{\pi}{6N} - \frac{7\pi^3}{360N^3} + \mathcal{O}(N^{-5}). \quad (5)$$

Since we want to focus on the low-lying excitations above the ground state, it is convenient to introduce a different labeling of the energies. Instead of labeling each energy by the whole set of momenta as in Eq. (3), we introduce a notation to distinguish between three different types of excitations, according to the distribution of the n_j with respect to the ground state. These labels refer to the true lattice states; their relation to the quantum numbers of the bosonic effective theory will be given in Sec. III.

(i) *Spin excitations.* The M outermost phases are removed and the remaining ones are again placed symmetrically and without vacancies around the origin, Fig. 1. We will distinguish these excitations by the total spin $S^z = \frac{N}{2} - M$. Due to spin-flip symmetry, the addition of M phases is energetically degenerate to the removal of M phases.

(ii) *Current excitations.* The whole set of numbers is shifted to the right or left by m integers, Fig. 2. We label these excitations by m , which we take to be positive (negative) if the shift is to the right (left).

(iii) *Particle-hole excitations* on top of the “zero-mode” spin and current excitations. These can always be described



FIG. 2. Sketch of a current excitation $m=1$. The shift of all phases can be either to the right, as depicted, or to the left. The left (right) Fermi points are denoted by $L(R)$, respectively.

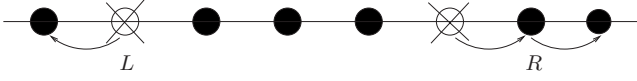


FIG. 3. Sketch of a particle-hole excitation labeled by $(1_L^L, 2_R^R)$. The arrows denote possible shifts in the position of the phases in order to create excitations. The excitations do not have to be symmetric: allowed are either shifts at the right or the left Fermi point or at both of them. The left (right) Fermi points are denoted by $L(R)$, respectively.

by a “shift” of occupied states relative to the filled Fermi sea,²¹ labeled by two sets of integers $\{m_n^L\}, \{m_n^R\}$, where $m_n^{L,R}$ denotes the number of Fermions that are shifted by n phases at the left (L) or right (R) Fermi point. A particular example is given in Fig. 3. These integers resemble bosonic occupation numbers but are so far used as unique labels for lattice eigenstates. The connection to the labels in the continuum bosonic field theory will be established in Sec. III.

In the following, we will label the energy levels by the set of numbers $(S^z, m, \{m_n^L\} \cup \{m_n^R\})$.

In the presence of zero-mode excitations only, the energy of the state with S^z -many particles removed from the ground state and of shifting all the phases by an integer m is obtained as

$$\begin{aligned} E(S^z, m, 0) - E_0 &= \left[\cos\left(\frac{\pi S^z}{N}\right) \cos\left(\frac{2m\pi}{N}\right) - 1 \right] E_0 \\ &= \frac{\pi}{N} \left[\frac{(S^z)^2}{2} + 2m^2 \right] \\ &\quad + \frac{\pi^3}{N^3} \left(\frac{(S^z)^2}{12} - \frac{(S^z)^4}{24} + \frac{m^2}{3} - \frac{2m^4}{3} - (mS^z)^2 \right) \\ &\quad + \mathcal{O}(N^{-5}). \end{aligned} \quad (6)$$

We now look at the particle-hole excitations, first with $S^z = m = 0$, and we assume that, at the left Fermi point, N_L -many phases are involved in the excitations. Let $j=0$ denote the leftmost phase in the ground state. Then the pattern of excitations is described by the set $\{j_1, \dots, j_{N_L}\}$, where each integer takes a value $j_i < N_L - 1$, including negative integers, and no two integers are equal. The analogous construction holds for the right Fermi point. The corresponding energy reads

$$E_0 + \sum_{j=0}^{N_L-1} \sin \frac{2j+1}{N} \pi - \sum_{\{j_1, \dots, j_{N_L}\}} \sin \frac{2j_i+1}{N} \pi + (L \leftrightarrow R). \quad (7)$$

By considering explicit excitations on a linear spectrum, it can be shown that in leading order in $1/N$ one obtains²¹

$$E(0, 0, \{m_n^L\} \cup \{m_n^R\}) - E_0 = \frac{2\pi}{N} \sum_{n=1}^{\infty} n(m_n^L + m_n^R) + \mathcal{O}(N^{-3}). \quad (8)$$

Corrections of $\mathcal{O}(N^{-3})$ cannot be written in terms of $\{m_n^L\} \cup \{m_n^R\}$ only, as will become clear in Sec. III. Most importantly, one sees that the above contributions (6) and (8) can be combined linearly in leading order,

$$\begin{aligned} E(S^z, m, \{m_n^L\} \cup \{m_n^R\}) - E_0 \\ = \frac{2\pi}{N} \left(\frac{(S^z)^2}{4} + m^2 + \sum_{n=1}^{\infty} n(m_n^L + m_n^R) \right) + \mathcal{O}(N^{-3}), \end{aligned} \quad (9)$$

and the higher-order terms $\mathcal{O}(N^{-3})$ contain nonlinear contributions where the excitations mix. These terms will be included on a more general footing in Sec. III.

The particle-hole contribution in Eq. (9) can be considered as the eigenvalue to the Hamiltonian $\sum_n n(a_n^{L\dagger} a_n^L + a_n^{R\dagger} a_n^R)$ with bosonic operators $[a_n^\nu, a_m^{\mu\dagger}] = \delta_{n,m} \delta_{\nu,\mu}$, where ν, μ can be R, L .^{15,21} However, due to the higher-order corrections in Eqs. (5), (6), and (9), the labels $(S^z, m, \{m_n^L\} \cup \{m_n^R\})$ introduced in this section are *not* the conventional bosonic occupation numbers. Hence the open question arises on what the linear combination of the bosonic eigenstates is that yields the original particle-hole eigenstates of the lattice model.

In Sec. III we will show that such mixings of bosonic states can be determined by taking into account higher-order corrections to Eq. (9) and finite interactions, $\Delta \neq 0$, if the one or other leads to a splitting of the corresponding energies.

B. Bethe ansatz solution

In this section, the exact BA solution for the spectrum of the XXZ Hamiltonian with $\Delta \neq 0$ is presented. With its help, we demonstrate how to use the notation for the excitations introduced in the previous section. For original references, we refer the reader to the book by Takahashi.¹⁴

The energy eigenvalues are parametrized by quasimomenta k_j as

$$E(\{k_j\}) = \frac{\Delta N}{4} - \Delta M - \sum_{j=1}^M \cos k_j.$$

This equation looks very similar to Eq. (3). Now, however, the $M = \frac{N}{2} - S^z$ quasimomenta k_j are solutions to the following coupled algebraic equations (Bethe equations):

$$e^{ik_j N} = (-1)^{M-1} \prod_{l \neq j}^M \frac{\exp[i(k_j + k_l)] + 1 + 2\Delta \exp[ik_j]}{\exp[i(k_j + k_l)] + 1 + 2\Delta \exp[ik_l]}. \quad (10)$$

The quasimomenta k_j pertain to interacting magnons above the ferromagnetic state. For numerical calculations it is more convenient to deal with the logarithmic version of these equations,

$$k_j N = 2\pi n_j + 2 \sum_{l \neq j}^M \arctan \frac{\Delta \sin[(k_j - k_l)/2]}{\cos[(k_j + k_l)/2] + \Delta \cos[(k_j - k_l)/2]}. \quad (11)$$

The lowest energy in the sector with $S^z = N/2 - M$ is given by a symmetric choice of the BA numbers in Eq. (11), such that

$$n_j = -\frac{M+1}{2} + j, \quad j = 1, \dots, M. \quad (12)$$

In the thermodynamic limit, the ground-state energy per lattice site, ε_0 , is given by

$$\varepsilon_0 = \begin{cases} \frac{\Delta}{4} - \frac{\sin \gamma}{\gamma} \int_{-\infty}^{\infty} \frac{\sinh(\pi/\gamma - 1)x}{2 \cosh x \sinh \pi x/\gamma} dx, & \Delta < 1, \\ \frac{1}{4} - \ln 2, & \Delta = 1, \end{cases} \quad (13)$$

where we defined γ by $\cos \gamma = \Delta$. We now want to obtain the energies of the lowest excitations directly from the BA equations. Some of these have been discussed in previous works.^{2,19,20,22} Our aim here is to perform a systematic study starting with very small interactions, $|\Delta| \ll 1$, and then to generalize these results to arbitrary values of Δ . The distribution of phases $\{n_j\}$ in Eq. (11) then defines one state uniquely.

We want to show how to use the labels for the eigenenergies, introduced in the previous section for $\Delta=0$, also in the interacting regime. As a motivation, let us first expand Eq. (11) to first order in Δ , i.e., close to the noninteracting point. This case can still be treated analytically. The corresponding quasimomenta are denoted by $k_j^{(0),(1)}$ and are given by

$$k_j^{(0)} = 2\pi \frac{n_j}{N},$$

$$k_j^{(1)} = k_j^{(0)} - 2\frac{\Delta}{N} \sum_l \frac{\sin[(k_j^{(0)} - k_l^{(0)})/2]}{\cos[(k_j^{(0)} + k_l^{(0)})/2]}. \quad (14)$$

This expansion relies on $\Delta e^{i(k_j^{(0)} - k_l^{(0)})/2} / \cos[(k_j^{(0)} + k_l^{(0)})/2] \ll 1$ and therefore has to be taken with care for values $k_j^{(0)} + k_l^{(0)} \approx \pm \pi$. One special case when this happens is near the Fermi points $k_j^{(0)} \approx k_l^{(0)} \approx \pm \pi/2$. That the expansion of the BA equations in the interaction parameter cannot be trusted near the Fermi points is well known from other BA solvable models.²³ However, global quantities which are obtained from summing over all Bethe numbers, such as the energy eigenvalues, turn out to be correct.^{8,23} More generally, the condition $k_j^{(0)} + k_l^{(0)} = \pi$ defines *critical pairs*,²⁴ with roots that can be either real or complex. The lowest excited states where these occur are current excitations in the $S^z=0$ sector and particle-hole excitations with $m_n^{L,R} = 1_2^{L,R}$, also in the $S^z=0$ sector. A careful analysis shows²⁴ that these critical pairs can lead to BA numbers different from the phases that one would calculate directly at $\Delta=0$. We illustrate this point in Appendix B for a few low-lying states in the chain with $N=8$, $\Delta=1$. However, for any finite Δ , one can still label uniquely each state by the distribution of phases given by $(S^z, m, \{m_n^L\} \cup \{m_n^R\})$ that one would obtain directly at $\Delta=0$, irrespective of the presence of critical pairs. This leads to general expressions for the energy levels to linear order in Δ .

Namely, the leading terms of the spin excitation energies to linear order in Δ are given by

$$E(S^z, 0, 0) - E_0 = \frac{\pi}{2N} \left(1 + \frac{4}{\pi} \Delta \right) (S^z)^2, \quad S^z = \frac{N}{2} - M. \quad (15)$$

For the lowest current excitations for $M=N/2$ one obtains the corresponding excitation energy in linear order

$$E(0, \pm 1, 0) - E_0 = \frac{2\pi}{N}, \quad (16)$$

which turns out to be unaffected by Δ in this order. Finally, the lowest particle-hole excitations have an energy

$$E(0, 0, \{m_n^L\} \cup \{m_n^R\}) - E_0 = \frac{2\pi}{N} \left(1 + \frac{2}{\pi} \Delta \right) \sum_n n(m_n^L + m_n^R). \quad (17)$$

From Eqs. (15)–(17) it is clear that $\Delta \neq 0$ generally lifts the degeneracy between the lowest particle-hole and current levels.

III. BOSONIZATION SOLUTION

In this section, we first review the leading order of the effective bosonic Hamiltonian for the low-energy excitations which is accurate within $\mathcal{O}(N^{-2})$. In the second part, next-leading corrections are included. The aim of this section is as follows: the eigenstates of the lattice model, $|S^z, m, \{m_n^L\} \cup \{m_n^R\}\rangle_L$, are labeled by phase configurations, as described above. On the other hand, as will be made clear below, the eigenstates of the effective model, $|S^z, m, \{m_n^L\} \cup \{m_n^R\}\rangle_B$, are labeled by the zero modes and bosonic occupation numbers as derived in Refs. 15 and 25, and shown in Eq. (22) below. Here, we wish to find those linear combinations of the bosonic states that yield the lattice eigenstates.

A. Leading order: noninteracting excitations

Using conventional bosonization, the leading contribution to an effective Hamiltonian, together with its eigenenergies and eigenstates, for the low-energy excitations of Eq. (1) has been derived.^{15,25} This Gaussian model reads

$$\Delta H_0 := \lim_{N \rightarrow \infty} (H - N\varepsilon_0) \frac{N}{2\pi v} + \frac{1}{12} \quad (18)$$

$$= \frac{1}{2} \left(\frac{\hat{Q}^2}{2\pi} + \frac{\hat{\Pi}^2}{2\pi} \right) + \sum_{n=1}^{\infty} n (a_n^{L\dagger} a_n^L + a_n^{R\dagger} a_n^R), \quad (19)$$

with eigenenergies

$$\begin{aligned} \Delta E_0(S^z, m, \{m_n^L\} \cup \{m_n^R\}) \\ = \lim_{N \rightarrow \infty} [E(S^z, m, \{m_n^L\} \cup \{m_n^R\}) - N\varepsilon_0] \frac{N}{2\pi v} + \frac{1}{12} \end{aligned} \quad (20)$$

$$= \frac{1}{2} [(S^z)^2/K + Km^2] + \sum_{n=1}^{\infty} n(m_n^L + m_n^R), \quad (21)$$

where ε_0 is the ground-state energy per lattice site, given in Eq. (13). The effective Hamiltonian and the energies carry an index $_0$ to indicate that they are the leading order in an asymptotic expansion for large N and small $\Delta E \ll 1/N$.

The eigenstates to Eq. (19) are given by

$$\begin{aligned} |S^z, m, \{m_n^L\} \cup \{m_n^R\}\rangle_B \\ = e^{i(\sqrt{(2\pi/K)S^z}\tilde{\varphi}_0 + \sqrt{2\pi Km}\varphi_0)} \prod_{n=1}^{\infty} (a_n^{L\dagger})^{m_n^L} (a_n^{R\dagger})^{m_n^R} |0\rangle, \end{aligned} \quad (22)$$

with the following commutation relations

$$\begin{aligned} [\varphi_0, \tilde{\varphi}_0] = -i; \quad [\hat{Q}, \tilde{\varphi}_0] = i; \quad [\hat{\Pi}, \varphi_0] = i; \\ [a_n^\mu, a_m^{\nu\dagger}] = \delta_{n,m} \delta_{\mu,\nu}, \end{aligned} \quad (23)$$

where μ, ν stand for the superscripts R, L .

The exponential in Eq. (22) creates the zero-mode excitations, labeled by the integers S^z, m . The product over bosonic operators in Eq. (22) creates bosonic excitations, where the numbers $m_n^{L,R}$ are the bosonic occupation numbers of the n th level. The constants used in Eqs. (18), (21), and (22) are

$$v = \frac{\pi \sqrt{1 - \Delta^2}}{2 \arccos \Delta}, \quad (24)$$

$$K = \frac{\pi}{\pi - \arccos \Delta}. \quad (25)$$

For weak interactions, $v = 1 + 2\Delta/\pi + \mathcal{O}(\Delta^2)$ and $K = 2 - 4\Delta/\pi + \mathcal{O}(\Delta^2)$, which, together with Eq. (21) agrees with Eqs. (15)–(17).

In this context, one should note again that in Eqs. (20) and (21) we used the same symbols as in Eqs. (6) and (8) and Eqs. (15)–(17) by which—in the asymptotical regime—we already identified those energies from the exact solution with the ones from bosonization. However, as stated above, the symbols have different meanings: for the lattice eigenstates, they encode the phase configurations, whereas for the bosonic states, they encode bosonic occupation numbers. In the asymptotical regime, the exact BA eigenstates are linear combinations of the states [Eq. (22)] in the degenerate subspaces. This will be made explicit in the following section.

B. Lifting of degeneracies due to irrelevant operators

The Hamiltonian in Eq. (19) constitutes the leading order in the large N limit. In the bosonization procedure, it results from taking account of spin-density and spin-current fluctua-

tions above the ground state, where forward and backward scattering processes are included. However, Umklapp scattering has been neglected so far. Furthermore, Eq. (19) relies on the linear dispersion approximation of excitations.

Umklapp scattering and nonlinear effects in the dispersion relation induce additional terms in the low-energy effective Hamiltonian. These terms are expressed through bosonic fields

$$\phi_R(x) = \phi_{R,0} + \hat{Q}_R \frac{x}{\ell} + \sum_{n=1}^{\infty} \frac{1}{\sqrt{4\pi n}} [e^{2\pi i n x/\ell} a_n^R + e^{-2\pi i n x/\ell} a_n^{R\dagger}], \quad (26)$$

$$\phi_L(x) = \phi_{L,0} + \hat{Q}_L \frac{x}{\ell} + \sum_{n=1}^{\infty} \frac{1}{\sqrt{4\pi n}} [e^{-2\pi i n x/\ell} a_n^L + e^{2\pi i n x/\ell} a_n^{L\dagger}], \quad (27)$$

$$\varphi(x) = \phi_R(x) + \phi_L(x), \quad (28)$$

where $\ell = Na$ is the length of the chain with a lattice constant a , which we choose as $a=1$. The operators encountered in Eqs. (19) and (23) are given by $\hat{Q} = \hat{Q}_R + \hat{Q}_L$, $\hat{\Pi} = \hat{Q}_R - \hat{Q}_L$, $\varphi_0 = \phi_{R,0} + \phi_{L,0}$, and $\tilde{\varphi}_0 = \phi_{R,0} - \phi_{L,0}$.

In the following, leading and next-leading Umklapp processes are encoded in operators $H_c^{(\nu)}$; leading band curvature effects are captured by an operator H_r .^{1,26} In our notation, these operators read

$$H_c^{(\nu)} = N \int_0^\ell \lambda_\nu \cos[\sqrt{8\pi K} \nu \varphi(x)] dx, \quad (29)$$

$$\begin{aligned} H_r = N \int_0^\ell dx \left\{ \lambda_+ \left(:(\partial_x \phi_R)^2: - \frac{\pi}{12N^2} \right) \left(:(\partial_x \phi_L)^2: - \frac{\pi}{12N^2} \right) \right. \\ \left. + \lambda_- \left[:(\partial_x \phi_R)^4: + \frac{b}{2\pi} :(\partial_x^2 \phi_R)^2: + (L \leftrightarrow R) \right. \right. \\ \left. \left. + \frac{1}{N^4} \left(\frac{\pi^2}{24} + \frac{\pi^2}{30} b \right) \right] \right\}, \end{aligned} \quad (30)$$

where ν is a positive integer and we defined $b = [3 - (1/K + K)]$. Operators in Eq. (30) with $::$ are normally ordered. Performing normal ordering in the corresponding expression in Ref. 1 yields the result (30). Especially, due to this normal ordering, the coefficient of the second derivative term is fixed by the b -dependent contribution to the ground-state energy, which is known from Ref. 1. For the leading operators $H_c^{(1)}, H_r$, the constants $\lambda_+, \lambda_-, \lambda_0$ are known¹

$$\lambda_+ = \frac{\Gamma(K)}{2\pi^2} \left(\frac{\Gamma(1 + 1/(2K - 2))}{2\sqrt{\pi}\Gamma(1 + K/(2K - 2))} \right)^{2K-2}, \quad (31)$$

$$\lambda_- = \frac{1}{12\pi K} \frac{\Gamma(3K/(2K - 2))\Gamma^3(1/(2K - 2))}{\Gamma(3/(2K - 2))\Gamma^3(K/(2K - 2))}, \quad (32)$$

$$\lambda_+ = \frac{1}{2\pi} \tan(\pi K / (2K - 2)). \quad (33)$$

The constant λ_1 is given with respect to the conformal field theory normalization,

$$\lim_{N \rightarrow \infty} \langle e^{i\alpha\varphi(x)} e^{-i\alpha\varphi(y)} \rangle = \frac{1}{|x - y|^{2d}}, \quad (34)$$

where

$$d = \frac{\alpha^2}{4\pi} \quad (35)$$

is the scaling dimension of the operator $e^{i\alpha\varphi}$. The expectation value in Eq. (34) is taken in the ground state.

In the following, we will calculate the contribution of the operators (29) and (30) in first-order perturbation theory. Before going into the details of the calculation, let us first discuss the different contributions that are to be expected from a perturbational treatment.

1. Scaling dimensions and perturbation theory

The scaling dimension d that governs the behavior of operators (19), (29), and (30) under renormalization group transformations can be read off from the exponent of two-point correlation functions such as Eq. (34). The fixed-point Hamiltonian (19) has scaling dimension $d=2$, whereas the scaling dimension of the leading Umklapp operator (29) is $d=2K$, see Eq. (35). The curvaturelike term (30) has scaling dimension $d=4$.

In first-order perturbation theory the correction to Eq. (21) from additional operators generally scales like $N^{-(d-2)}$ for finite N . Thus operators (29) and (30) can induce additional term scaling like N^{-2} , $N^{-(2K-2)}$, respectively.

On top of these leading contributions, next-leading terms exist. On the one hand, these stem from second-order perturbation theory, giving rise, for example, to terms scaling like N^{-4} , $N^{-(4K-4)}$. On the other hand, higher-order operators can contribute in first-order perturbation theory. For example, the second-order Umklapp operator can yield a term $\sim N^{-(8K-2)}$. Generally, any additional operator can create terms in any perturbational order. We illustrate the exponents of the first few leading contributions in Fig. 4.

Note that at special values of Δ , the exponents cross. At the free fermion point $\Delta=0$ the amplitudes of the Umklapp operators vanish. However, a nontrivial crossover happens at $\Delta=1/2$. Here, the leading exponent of second-order perturbation theory in H_c , $4K-4$, crosses with the exponent 2 stemming from H_r . At this crossover point, the two algebraic corrections merge to form a logarithmic contribution.^{1,27} The same happens for higher orders. At the crossover points that are given by roots of unity, $\Delta = \cos \frac{\pi}{n}$, $n > 2$ integer, nontrivial degeneracies between excited levels persist. At these points, the XXZ model has an invariance under the loop algebra sl_2 , leading to additional degeneracies.²⁸ An unambiguous treatment of these special points has been derived within the BA.²⁹⁻³¹ In Appendix A, we illustrate how these degeneracies show up for the eigenvalues of the Gaussian model, Eq. (21), by sketching the conformal towers at $\Delta=0, 1/2, 1$.

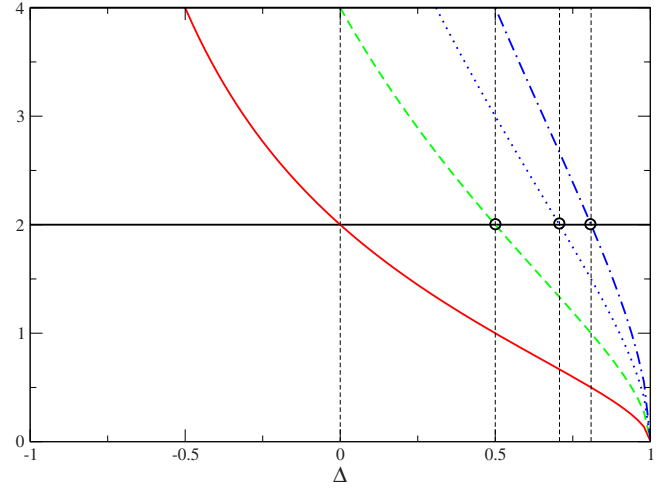


FIG. 4. (Color online) The exponents 2, 4 (horizontal black lines), $2K-2$ (red), $4K-4$ (green dashed), $6K-6$ and $8K-8$ (blue dotted and dotted-dashed, respectively). The vertical dashed black lines are at the values $\Delta = \cos \frac{\pi}{2}, \cos \frac{\pi}{3}, \cos \frac{\pi}{4}, \cos \frac{\pi}{5}$. The open circles denote the points where logarithmic contributions occur.

We shortly comment on the isotropic case. Obviously, the distinction between leading and next-leading corrections from Umklapp operators does not make sense for the isotropic point, $\Delta=1$. Here, all exponents $2\nu K - 2\nu \rightarrow 0$, and the scaling dimension of $H_c^{(1)}$ is two at that point. RG studies^{1,2,32} have shown that the corrections ΔE_1 to the levels ΔE_0 read

$$\Delta E_1(0,0,0) - \Delta E_0(0,0,0) = -\frac{3}{8 \ln^3 N}, \quad (36)$$

$$\Delta E_1(0, \pm 1, 0) - \Delta E_0(0, \pm 1, 0) = \frac{g_{\pm}}{\ln N}, \quad (37)$$

$$\Delta E_1(\pm 1, 0, 0) - \Delta E_0(\pm 1, 0, 0) = \frac{g_1}{\ln N}. \quad (38)$$

The amplitude g_1 is known exactly while for the amplitudes g_{\pm} , numerical calculations were performed.²

In the following, we will concentrate on the first-order contributions of operators (29) and (30). Especially, we will show that the operator $H_c^{(m)}$ leads to the symmetric/antisymmetric combination of states with $\pm|m|$ and lifts their degeneracy in first-order perturbation theory if $S^z=0$. The corrections to Eq. (21) are then of order N^{2-2Km^2} . In all other cases, this operator only contributes in *second-order* perturbation theory, yielding corrections to Eq. (21) of order N^{4-4Km^2} . Operator (30) always contributes in first-order perturbation theory, resulting into corrections $\sim N^{-2}$.

2. First-order contributions from Umklapp operators

Let us first consider the zero-mode states $|S^z, m, m_n^L = m_n^R = 0\rangle_{B,L}$, constructed according to Eq. (22). By inserting the mode expansions (26)–(28) into Eq. (29) for the leading Umklapp operator $H_c^{(1)}$, one calculates the expectation values of this operator between the zero-mode excited states. Using the

commutation relations (23) one can show that

$${}_B\langle 0, 1, 0 | H_c^{(1)} | 0, 1, 0 \rangle_B = 0, \quad {}_B\langle 0, 1, 0 | H_c^{(1)} | 0, -1, 0 \rangle_B = C, \quad (39)$$

$${}_B\langle 0, -1, 0 | H_c^{(1)} | 0, -1, 0 \rangle_B = 0, \quad {}_B\langle 0, -1, 0 | H_c^{(1)} | 0, 1, 0 \rangle_B = C, \quad (40)$$

with

$$C = -(2\pi)^{2K} \lambda_1 N^{1-2K}. \quad (41)$$

The corresponding eigenstates in this order are

$$|0, 1, 0\rangle_L = \frac{1}{\sqrt{2}}(|0, 1, 0\rangle_B + |0, -1, 0\rangle_B),$$

$$|0, -1, 0\rangle_L = \frac{1}{\sqrt{2}}(|0, 1, 0\rangle_B - |0, -1, 0\rangle_B),$$

where the labels of the lattice eigenstates have been chosen according to the discussions in Sec. II B and Ref. 24. Thus

$$\Delta E_1(0, 1, 0) = -(2\pi)^{2K} \lambda_1 N^{1-2K}, \quad (42)$$

$$\Delta E_1(0, -1, 0) = (2\pi)^{2K} \lambda_1 N^{1-2K}. \quad (43)$$

Consequently, the leading operator describing Umklapp scattering lifts the degeneracy between the $|m|=1$ states for $S^z=0$ and $m_n^L = m_n^R = 0$, such that the symmetric combination is energetically lower than the antisymmetric combination.

Within the BA, the interacting quasiparticles above the antiferromagnetic ground state are spinons.^{22,33} Comparing the symmetric and antisymmetric current excitations with the energies of the lowest $S^z=0$ two-spinon states from the BA,^{2,24} we conclude that the symmetric (antisymmetric) combination of current excitations corresponds to the lowest two-spinon triplet (singlet) state with $S^z=0$.

Particle-hole excitations at $|m|=1$ can be included as well. To determine the expectation values of the Umklapp operator $H_c^{(1)}$ in Eq. (29) between these states, one again uses Eq. (22) together with commutation relations (23). This results in

$$|0, 1, 1_1^{R,L}\rangle_L = \frac{1}{\sqrt{2}}(|0, 1, 1_1^{R,L}\rangle_B + |0, -1, 1_1^{R,L}\rangle_B), \quad (44)$$

$$|0, -1, 1_1^{R,L}\rangle_L = \frac{1}{\sqrt{2}}(|0, 1, 1_1^{R,L}\rangle_B - |0, -1, 1_1^{R,L}\rangle_B), \quad (45)$$

with energy contributions

$$\Delta E_1(0, \pm 1, 1_1^{R,L}) = (1 - 2K)\Delta E_1(0, \pm 1, 0), \quad (46)$$

$$\Delta E_1(0, \pm 1, 1_1^R 1_1^L) = (1 - 2K)^2 \Delta E_1(0, \pm 1, 0), \quad (47)$$

where the two particle-hole excitations are taken into account in the second equation. The lattice eigenstates are again the symmetric and antisymmetric combinations of the bosonic eigenstates in this order.

Let us now consider the states $|1, \pm 1, 0\rangle_B$, that is, states with one spinlike and one currentlike excitation. Proceeding

similarly as we did in order to arrive at Eqs. (42) and (43) but now including the additional spin excitation, we find

$${}_B\langle 1, 1, 0 | H_c^{(1)} | 1, 1, 0 \rangle_B = 0, \quad {}_B\langle 1, 1, 0 | H_c^{(1)} | 1, -1, 0 \rangle_B = 0, \quad (48)$$

$${}_B\langle 1, -1, 0 | H_c^{(1)} | 1, -1, 0 \rangle_B = 0, \quad {}_B\langle 1, -1, 0 | H_c^{(1)} | 1, 1, 0 \rangle_B = 0. \quad (49)$$

Especially, the terms in the second equations in Eqs. (48) and (49) now vanish due to the finite magnetization. This argument can be generalized to arbitrary $S^z \neq 0$. Thus we conclude that for states carrying currentlike $|m|=1$ and spinlike excitations, the Umklapp operators $H_c^{(p)}$ contribute in *second-order* perturbation theory only.

The same is true for states without zero mode but bosonic excitations only. If these states are degenerate with respect to the Hamiltonian (19), these degeneracies are not lifted by $H_c^{(1)}$ in first-order perturbation theory. However, second-order perturbation theory generally yields a finite contribution and can thus lead to a lifting of those degeneracies.

3. First-order contributions from curvaturelike terms

The operator H_r in Eq. (30) yields a finite contribution for all states in first-order perturbation theory. It will generally split the degenerate bosonic levels with the same excitation energy. In particular, we obtain for the lowest levels by a straightforward evaluation of the expectation values

$$\Delta E_1(0, 0, 0) = -\frac{\pi^2}{720} [5\lambda_+ + 6(5 + 4b)\lambda_-] N^{-2}, \quad (50)$$

$$\Delta E_1(0, 0, 1_1^{R,L}) = \Delta E_1(0, 0, 0) + \frac{\pi^2}{6} [\lambda_+ + 6(1 - 4b)\lambda_-] N^{-2}, \quad (51)$$

$$\Delta E_1(0, 0, 1_2^{R,L}) = \Delta E_1(0, 0, 0) + \frac{\pi^2}{3} [\lambda_+ - 6(5 + 4b)\lambda_-] N^{-2}, \quad (52)$$

$$\Delta E_1(0, 0, 2_1^{R,L}) = \Delta E_1(0, 0, 0) + \frac{\pi^2}{3} [\lambda_+ + 6(1 - 16b)\lambda_-] N^{-2}, \quad (53)$$

$$\Delta E_1(0, 0, 1_1^R 1_1^L) = \Delta E_1(0, 0, 0) - \frac{\pi^2}{3} [11\lambda_+ - 6(1 - 4b)\lambda_-] N^{-2}, \quad (54)$$

$$\Delta E_1(1, 0, 0) = \frac{\pi^2}{720} \left[5 \left(\frac{1}{K} - 6 \right)^2 \lambda_+ + \frac{6}{K^2} (60 - 60K + (5 + 4b)K^2) \lambda_- \right] N^{-2}, \quad (55)$$

$$\Delta E_1(1,0,1_1^{R,L}) = \Delta E_1(1,0,0) - \pi^2 \left[\lambda_+ \left(\frac{1}{K} - \frac{1}{6} \right) + \left(\frac{6}{K} - (1-4b) \right) \lambda_- \right] N^{-2}, \quad (56)$$

$$\Delta E_1(1,0,1_2^{R,L}) = \Delta E_1(1,0,0) + \frac{\pi^2}{3K} \{ (1-6/K) \lambda_+ + [18\sqrt{8K+(1-2b)^2K^2} - (36+12K+60bK)] \lambda_- \} N^{-2}, \quad (57)$$

$$\Delta E_1(1,0,2_1^{R,L}) = \Delta E_1(1,0,0) + \frac{\pi^2}{3K} \{ (1-6/K) \lambda_+ - [18\sqrt{8K+(1-2b)^2K^2} + (36+12K+60bK)] \lambda_- \} N^{-2}, \quad (58)$$

$$\Delta E_1(1,0,1_1^R 1_1^L) = \Delta E_1(1,0,0) - \frac{\pi^2}{3K} \{ (6+11K) \lambda_+ + [36+6(4b-1)K] \lambda_- \} N^{-2}, \quad (59)$$

with $b=3-(1/K+K)$. In this order of N^{-2} , with $1/2 > \Delta \neq 0$ fixed, the corresponding eigenstates are

$$|0,0,0\rangle_L = |0,0,0\rangle_B, \quad (60)$$

$$|0,0,1_1^{R,L}\rangle_L = |0,0,1_1^{R,L}\rangle_B, \quad (61)$$

$$|0,0,1_2^{R,L}\rangle_L = |0,0,1_2^{R,L}\rangle_B, \quad (62)$$

$$|0,0,2_1^{R,L}\rangle_L = |0,0,2_1^{R,L}\rangle_B, \quad (63)$$

$$|0,0,1_1^R 1_1^L\rangle_L = |0,0,1_1^R 1_1^L\rangle_B, \quad (64)$$

$$|1,0,0\rangle_L = |1,0,0\rangle_B, \quad (65)$$

$$|1,0,1_1^{R,L}\rangle_L = |1,0,1_1^{R,L}\rangle_B, \quad (66)$$

$$|1,0,1_1^R 1_1^L\rangle_L = |1,0,1_1^R 1_1^L\rangle_B. \quad (67)$$

Thus for the above low-lying levels, the lattice eigenstates are just the bosonic eigenstates. However, the bosonic states have to be combined appropriately to yield the correct lattice eigenstates for the following levels:

$$|1,0,1_2^{R,L}\rangle_L = \cos \alpha |1,0,1_2^{R,L}\rangle_B + \sin \alpha |1,0,2_1^{R,L}\rangle_B, \quad (68)$$

$$|1,0,2_1^{R,L}\rangle_L = -\sin \alpha |1,0,1_2^{R,L}\rangle_B + \cos \alpha |1,0,2_1^{R,L}\rangle_B, \quad (69)$$

$$\tan \alpha = \frac{\sqrt{(2b-1)^2 + 8/K} + (2b-1)}{\sqrt{(2b-1)^2 + 8/K} - (2b-1)}. \quad (70)$$

In complete analogy, the effect of H_r in Eq. (30) on the current-carrying states with $|m|=1$ can be treated. For example,

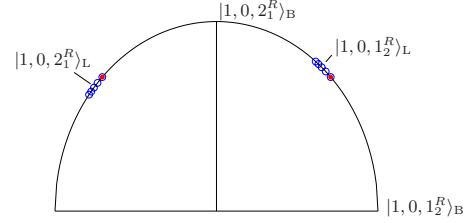


FIG. 5. (Color online) Mixing of bosonic states according to Eqs. (68) and (69). The circles denote the lattice eigenstates for $\Delta=0,0.1,\dots,0.4$. The red dots are the symmetric and antisymmetric combinations for $\Delta=0$.

$$E_1(1, \pm 1, 0) = \pm \frac{\pi^2}{720} \left[5 \left(2 - \frac{3}{K} \right) \left(3 - \frac{2}{K} \right) [6 + K(11 + 6K)] \lambda_+ + \frac{6}{K^2} \{ 60 - 60K + K^2 [365 + 4b + 60K(K-1)] \} \lambda_- \right] N^{-2}, \quad (71)$$

$$|1, \pm 1, 0\rangle_L = |1, \pm 1, 0\rangle_B. \quad (72)$$

An important consistency check of Eqs. (50)–(59) is the limit $\Delta=0$. In this case, $K=2$, $b=1/2$, $\lambda_+=0$, and $\lambda_- = 1/6$. Then the above corrections yield those obtained in Eqs. (5)–(7). (Note that the above energy correction has to be multiplied by $2\pi v/N$ to obtain the contribution to the total energy.) The mixing of states in Eqs. (68) and (69) is illustrated in Fig. 5.

In the BA solution, energy (52) is encoded by a complex string, which makes a finite-size analysis, especially for large N , difficult. Result (52) gives the leading nonuniversal contribution to this energy analytically, avoiding any problems with strings.

Let us now look at the lattice states $|0,0,1_2^{R,L}\rangle_L$, $|0,0,2_1^{R,L}\rangle_L$ on the one hand and $|1,0,1_2^{R,L}\rangle_L$, $|1,0,2_1^{R,L}\rangle_L$ on the other hand. The corresponding lattice and bosonic eigenstates are given in Eqs. (62), (63), (68), and (69), respectively. For $S^z=1$, the two bosonic states $|1,0,1_2^{R,L}\rangle_B$, $|1,0,2_1^{R,L}\rangle_B$ are mixed due to H_r with the rotation angle given in Eq. (70). This angle tends to $\pi/4$ in the limit $\Delta \rightarrow 0$, such that Eqs. (68) and (69) are the antisymmetric and symmetric combinations, respectively. A similar mixing was found from numerics for the model (1) with hard wall boundary conditions.⁹

Surprisingly, in this order, the analogous bosonic states for $S^z=0$ [Eqs. (62) and (63)] do *not* mix for a given interaction $1/2 > \Delta \neq 0$. The bosonization procedure directly at $\Delta=0$ constructs fermionic states on the lattice that are the symmetric and antisymmetric combinations of the corresponding bosonic states.²¹ However, at $\Delta=0$, $|0,0,1_2^{R,L}\rangle_L$ and $|0,0,2_1^{R,L}\rangle_L$ are exactly degenerate, as can be seen from Eq. (7), such that any combination of them is allowed. A finite interaction lifts this degeneracy but does not mix their bosonic equivalents in first order of H_r , H_1 .

We summarize the above results for the excitation energies and give their scaling behaviors, including the leading perturbational corrections.

$$\begin{aligned} \Delta E_1(0, \pm 1, \{m_n^L\} \cup \{m_n^R\}) &= c_c^{(1)}(0, \pm 1, m_n^L, m_n^R) N^{2-2K} \\ &+ c_r(0, \pm 1, m_n^L, m_n^R) N^{-2} \\ &+ c_c^{(2)}(0, \pm 1, m_n^L, m_n^R) N^{4-4K}, \end{aligned} \quad (73)$$

$$\begin{aligned} \Delta E_1(0, 0, \{m_n^L\} \cup \{m_n^R\}) &= c_r(0, 0, m_n^L, m_n^R) N^{-2} \\ &+ c_c^{(2)}(0, 0, m_n^L, m_n^R) N^{4-4K}, \end{aligned} \quad (74)$$

$$\begin{aligned} \Delta E_1(\pm 1, m, \{m_n^L\} \cup \{m_n^R\}) &= c_r(\pm 1, m, m_n^L, m_n^R) N^{-2} \\ &+ c_c^{(2)}(\pm 1, m, m_n^L, m_n^R) N^{4-4K}, \end{aligned} \quad (75)$$

where in the last equation $m=0, \pm 1$. The terms $c_r, c_c^{(1)}$ are due to first-order contributions from $H_r, H_c^{(1)}$, and have been calculated in Eqs. (42), (43), (46), (47), (50)–(59), and (71) for the lowest states. Along that way, they can be determined for any state. The terms $c_c^{(2)}$ stem from second-order contributions in H_c and are not considered in this work. For the ground state at given S^z , this contribution was determined in Ref. 1.

Therefore, the low-energy eigenvalues of the Heisenberg chain can be calculated for $\Delta < 1/2$ including the order $N^{-\max(4, 2K)}$ without using the BA and thus avoiding strings completely.

IV. NUMERICAL RESULTS

For those states listed in Appendix B, we performed a systematic finite-size scaling analysis up to lattice lengths of $N=2 \times 10^3$ in order to confirm our results (42)–(47), (50)–(59), and (71).

In Fig. 6, we compare the field-theoretical results for a few energies with BA data as a function of the system length N for $\Delta=0.2$. As illustrative examples, we take two current-carrying excitations, Eqs. (42) and (43), and the bosonic states, Eqs. (50)–(59), in the sectors with $S^z=0, 1$.

For $S^z=0$, the different exponents of finite-size contributions to the energies of current-carrying excitations compared to states with bosonic excitations only are clearly discernible, see the left panel of Fig. 6. On the other hand, for $S^z=1$, the leading finite-size corrections to both current and bosonic excitations scale with the same exponent, as shown in the right panel of Fig. 6.

For all states, the agreement is almost perfect for the longest chains studied. We also give the field-theoretical result for one particle-hole energy which belongs to a complex string in the BA. The field-theoretical prediction is independent of the actual position of roots and thus avoids any convergence problems of complex string solutions in the finite-size scaling analysis.

In order to estimate the agreement quantitatively, we show the relative deviation in Fig. 7. The plots show relative deviations of the order of 10^{-2} for $N \sim 10$, going down to

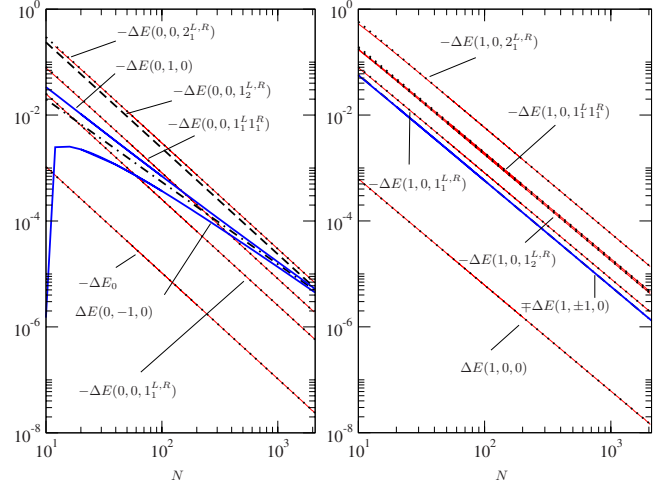


FIG. 6. (Color online) Comparison of the bosonic eigenlevels [Eqs. (50)–(59)] (dotted black) with the BA values for the corresponding particle-hole excitations (straight red) as a function of N for $\Delta=0.2$. In the left panel, $S^z=0$ and $S^z=1$ in the right panel. The black dashed line in the left panel is the field-theoretical prediction for an energy given by a string solution in the BA. Also shown (fat blue lines) are current excitations. The dotted-dashed line in the left panel is the field-theoretical result (43). The field-theoretical result (71) in the right panel cannot be distinguished from the numerical data.

roughly 10^{-3} for $N \sim 100$. This trend continues, and for $N \sim 2000$, the relative deviation is around 10^{-4} for the energies considered here.

For $\Delta > 1/2$, the first term in the energies of current-carrying excitations [Eq. (73)] still is leading with its exponent $2-2K$, as illustrated in Fig. 4. On the other hand, higher-order terms with exponent $4-4K$ are given by Umklapp processes in second-order perturbation theory. We confirmed the exponents by performing numerical finite-size scaling for $\Delta=3/4$ as well. However, the analytical calcula-

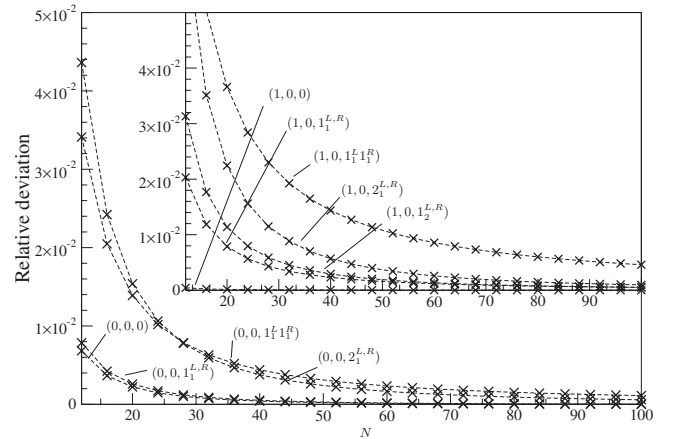


FIG. 7. Relative deviation of the bosonic eigenlevels (50)–(59), except for Eq. (52), from the BA values, for different ring lengths N . The large graph refers to $S^z=0$ levels, whereas the inset shows $S^z=1$ levels. The dashed lines are guides to the eye.

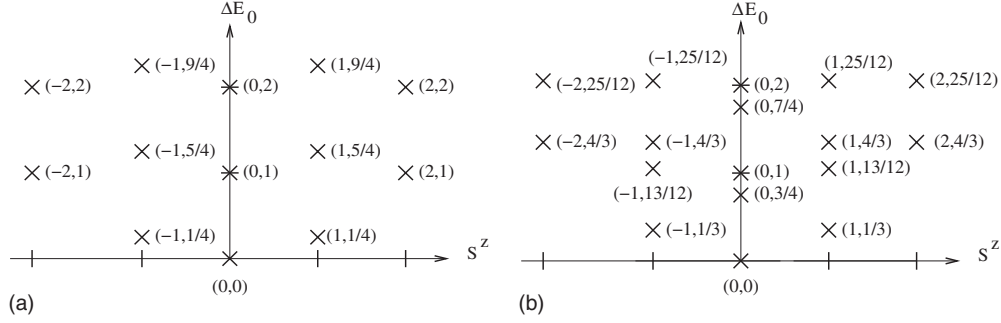


FIG. 8. The lowest excitations for $\Delta=0$ ($\Delta=1/2$) in the left (right) panel. The energies corresponding to the crosses in the $(S^z, \Delta E_0)$ plane are given in Eqs. (A1) and (A2), respectively.

tion of the corresponding coefficients is out of the scope of this paper.

V. CONCLUSION

We have calculated the coefficients of an asymptotic expansion in the inverse system length of a large number of low-lying excited energies. This calculation does not employ the BA directly, and thus avoids complex strings which are difficult to deal with numerically. Instead, operators (29) and (30) have to be diagonalized which involves the use of bosonic commutation relations only. This scheme is particularly useful for $\Delta < 1/2$, where the energies are determined analytically within an accuracy including $\mathcal{O}(N^{-\max(4, 2K)})$. For the lowest ~ 50 eigenlevels that we have checked, no degeneracies remain that have not been already present in the lattice model.

As a further outcome, the lattice eigenstates are expressed in terms of bosonic modes, again within the accuracy given above, for a fixed Δ . This representation of eigenstates is different from the BA representation of eigenstates.

So far, we have demonstrated that our method works fine when the number of bosonic quasiparticles is kept fixed and the system size enters as a parameter. In order to make contact to recent calculations of the dynamical structure factor^{8,34,35} and other dynamical quantities^{36,37} from numerically solving the BA equations, one would have to decompose states of fixed total momentum into the bosonic states. In how far our method could prove useful here to obtain both numerical and even analytical results for form factors restricted to low excitation energies in the Heisenberg spin chain is an important point for future research. The interest in these quantities is high, as underlined by the most recent work³⁸ where the expectation value of the local magnetization between the ground state and a current-carrying state was computed.

A further interesting open question concerns the isotropic case, $\Delta=1$. Corrections to the leading finite-size scaling of bosonic excited states have not been studied yet for this model. One expects logarithmic contributions in this case, as in Eqs. (36)–(38). The determination of both the exponents and the prefactors of the logarithms requires setting up RG equations for the individual energy levels which we will leave as a task for future investigations.

ACKNOWLEDGMENTS

We thank F.H.L. Essler, S. Reyes, and A. Struck for helpful discussions. Financial support from the Transregional Collaborative Research Centre SFB/TRR 49 of the Deutsche Forschungsgemeinschaft and the MATCOR school of excellence is gratefully acknowledged. M.B. also acknowledges financial support from the European science network INSTANS and hospitality at the Rudolf-Peierls-Centre for Theoretical Physics at the University of Oxford, where part of this work has been carried out.

APPENDIX A: CONFORMAL TOWERS FOR $\Delta=0, 1/2, 1$

In this appendix, we illustrate the low-energy spectra [Eq. (21)] for $\Delta=0, 1/2, 1$ in an $S^z - \Delta E_0$ diagram (conformal tower). On the one hand, this shows the lifting of degeneracies at finite Δ compared to the $\Delta=0$ case. On the other hand, it demonstrates the occurrence of nontrivial symmetries at the special points $\Delta=1/2=\cos\frac{\pi}{3}$ and $\Delta=1$.

Each cross in a conformal tower is labeled by its coordinates in the $(S^z, \Delta E_0)$ plane. The corresponding quantum numbers $(S^z, m, \{m_n^L\} \cup \{m_n^R\})$ of the bosonic field theory are listed in the following.

For $\Delta=0$, cf. Fig. 8(a):

$$\begin{aligned}
 (0, 1): & \quad (0, 0, 1_1^L), (0, 0, 1_1^R), (0, \pm 1, 0), \\
 (0, 2): & \quad (0, 0, 1_1^L 1_1^R), (0, 0, 2_1^L), (0, 0, 2_1^R), (0, 0, 1_2^R), (0, 0, 1_2^L), \\
 & \quad (0, \pm 1, 1_1^L), (0, \pm 1, 1_1^R), \\
 (\pm 1, 1/4): & \quad (\pm 1, 0, 0), \\
 (\pm 1, 5/4): & \quad (\pm 1, 0, 1_1^L), (\pm 1, 0, 1_1^R), (\pm 1, \pm 1, 0), \\
 (\pm 1, 9/4): & \quad (\pm 1, 0, 1_1^L 1_1^R), (\pm 1, 0, 2_1^L), (\pm 1, 0, 2_1^R), (\pm 1, 0, 1_2^L), \\
 & \quad (\pm 1, 0, 1_2^R), (\pm 1, \pm 1, 1_1^L), (\pm 1, \pm 1, 1_1^R), \\
 (\pm 2, 1): & \quad (\pm 2, 0, 0), \\
 (\pm 2, 2): & \quad (\pm 2, 0, 1_1^L), (\pm 2, 0, 1_1^R), (\pm 2, \pm 1, 0). \tag{A1}
 \end{aligned}$$

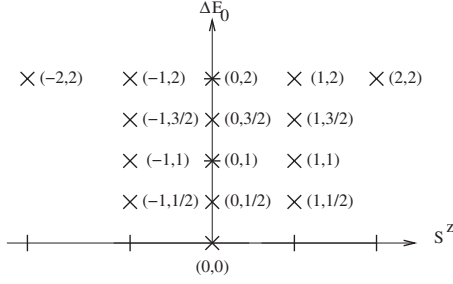


FIG. 9. The lowest excitations for $\Delta=1$. The energies corresponding to the crosses in the $(S^z, \Delta E_0)$ plane are given in Eq. (A3).

For $\Delta=1/2$, cf. Fig. 8(b):

$$(0, 3/4): (0, \pm 1, 0),$$

$$(0, 1): (0, 0, 1_1^L), (0, 0, 1_1^R),$$

$$(0, 7/4): (0, \pm 1, 1_1^L), (0, \pm 1, 1_1^R),$$

$$(0, 2): (0, 0, 1_1^L 1_1^R), (0, 0, 2_1^L), (0, 0, 2_1^R), (0, 0, 1_2^L), (0, 0, 1_2^R),$$

$$(\pm 1, 1/3): (\pm 1, 0, 0),$$

$$(\pm 1, 13/12): (\pm 1, \pm 1, 0),$$

$$(\pm 1, 4/3): (\pm 1, 0, 1_1^L), (\pm 1, 0, 1_1^R),$$

$$(\pm 1, 25/12): (\pm 1, \pm 1, 1_1^L), (\pm 1, \pm 1, 1_1^R),$$

$$(\pm 2, 4/3): (\pm 2, 0, 0),$$

$$(\pm 2, 25/12): (\pm 2, \pm 1, 0). \quad (\text{A2})$$

For $\Delta=1$, cf. Fig. 9:

$$(0, 1/2): (0, \pm 1, 0),$$

$$(0, 1): (0, 0, 1_1^L), (0, 0, 1_1^R);$$

$$(0, 3/2): (0, \pm 1, 1_1^L), (0, \pm 1, 1_1^R);$$

$$(0, 2): (0, 0, 1_1^L 1_1^R), (0, 0, 2_1^L), (0, 0, 2_1^R), (0, 0, 1_2^L), (0, 0, 1_2^R), \\ (0, \pm 2, 0);$$

$$(\pm 1, 1/2): (\pm 1, 0, 0);$$

$$(\pm 1, 1): (\pm 1, \pm 1, 0);$$

$$(\pm 1, 3/2): (\pm 1, 0, 1_1^L), (\pm 1, 0, 1_1^R);$$

$$(\pm 1, 2): (\pm 1, \pm 1, 1_1^L), (\pm 1, \pm 1, 1_1^R);$$

$$(\pm 2, 2): (\pm 2, 0, 0) \quad (\text{A3})$$

APPENDIX B: LOW ENERGY STATES FOR THE XXX CHAIN WITH $N=8$ LATTICE SITES

In Table I, a few low-lying excited states above the ground state (note the $\pm S^z$ symmetry) are given for the XXX chain with eight lattice sites. The BA numbers are given as well as the quasimomenta and the lattice labels, according to Section B. For excitations with purely real quasimomenta, that is, for phases $|n_j| < n_c$ with $n_c = (S^z + N/2)/2$, there are no convergence problems in the finite-size scaling analysis because all quasimomenta are real.²⁴ Otherwise, string solutions occur, which have to be treated separately. The stars * symbolize the occurrence of such solutions, where a critical pair forms either a real or a complex string. These are separated off from the BA equations. Reference 24 shows how to assign BA numbers to these critical pairs as well. Our results for the excited states agree with those published in Ref. 39, where a different parametrization was chosen.

TABLE I. Labeling of the BA levels for $\Delta=1$ and $N=8$.

E	S^z	$2n_j$				k_j				Lattice label
-3.65109	0	-3	-1	1	3	-1.61959	-0.506761	0.506761	1.61959	(0,0,0)
-3.12842	0	-1	1	*	*	0	π	-0.971321	0.971321	(0,1,0)
-3.12842	1	-2	0	2		-0.971321	0	-0.971321		(1,0,0)
-2.69963	0	-1	1	*	*	$\frac{\pi}{2} + i\infty$	$\frac{\pi}{2} - i\infty$	-0.555164	0.555164	(0,-1,0)
-2.45874	0	∓ 3	∓ 1	∓ 1	± 5	$\pm \pi$	± 0.214056	± 0.738788	± 1.83146	$(0, 0, 1_1^{R,L})$
-2.45874	1	0	∓ 2	± 4		∓ 0.214056	± 0.738788	± 1.83146		$(1, \pm 1, 0)$
-2.14515	1	∓ 2	0	± 4		∓ 1.04767	∓ 0.0951988	± 1.92827		$(1, 0, 1_1^{R,L})$
-2.14515	0	∓ 5	∓ 3	∓ 1	± 3	$\mp \pi$	∓ 1.04767	∓ 0.0951988	± 1.92827	$(0, \mp 1, 1_1^{R,L})$
-1.85464	0	∓ 3	∓ 1	∓ 3	± 5	∓ 1.87588	∓ 0.794255	± 1.09933	$\pm \pi$	$(0, 0, 2_1^{R,L})$
-1.85454	1	∓ 2	∓ 2	± 4		∓ 1.09933	± 0.794255	± 1.87588		$(1, \mp 1, 1_1^{R,L})$
-1.80194	2	-1	1			-0.448799	0.448799			(2,0,0)
-1.80194	0	-5	-1	1	5	$-\pi$	-0.448799	0.448799	π	$(0, 0, 1_1^L 1_1^R)$
-1.80194	1	0	∓ 2	± 6		∓ 0.448799	± 0.448799	$\pm \pi$		$(1, \pm 1, 1_1^{R,L})$

*bortz@physik.uni-kl.de

- ¹S. Lukyanov, Nucl. Phys. B **522**, 533 (1998).
- ²I. Affleck, D. Gepner, H. Schulz, and T. Ziman, J. Phys. A **22**, 511 (1989).
- ³T. Ami, M. K. Crawford, R. L. Harlow, Z. R. Wang, D. C. Johnston, Q. Huang, and R. W. Erwin, Phys. Rev. B **51**, 5994 (1995).
- ⁴N. Motoyama, H. Eisaki, and S. Uchida, Phys. Rev. Lett. **76**, 3212 (1996).
- ⁵M. Bockrath, D. H. Cobden, J. Lu, A. Rinzler, R. E. Smalley, L. Balents, and P. L. McEuen, Nature (London) **397**, 598 (1999).
- ⁶H. Ishii *et al.*, Nature (London) **426**, 540 (2003).
- ⁷J. Lee, S. Eggert, H. Kim, S. J. Kahng, H. Shinohara, and Y. Kuk, Phys. Rev. Lett. **93**, 166403 (2004).
- ⁸R. G. Pereira, J. Sirker, J. S. Caux, R. Hagemans, J. M. Maillet, S. R. White, and I. Affleck, Phys. Rev. Lett. **96**, 257202 (2006); J. Stat. Mech.: Theory Exp. (2007) P08022.
- ⁹I. Schneider, A. Struck, M. Bortz, and S. Eggert, Phys. Rev. Lett. **101**, 206401 (2008).
- ¹⁰H. Bethe, Z. Phys. **71**, 205 (1931).
- ¹¹L. Hulthen, Ark. Mat., Astron. Fys. **26A**, 1 (1938).
- ¹²J. des Cloizeaux and M. Gaudin, J. Math. Phys. **7**, 1384 (1966).
- ¹³C. Yang and C. Yang, Phys. Rev. **150**, 321 (1966).
- ¹⁴M. Takahashi, *Thermodynamics of One-Dimensional Solvable Problems* (Cambridge University Press, New York, 1999).
- ¹⁵I. Affleck, in *Fields, Strings and Critical Phenomena*, edited by E. Brézin and J. Zinn-Justin (North Holland, Amsterdam, 1990), p. 563.
- ¹⁶J. L. Cardy, J. Phys. A **17**, L385 (1984).
- ¹⁷J. L. Cardy, J. Phys. A **17**, L961 (1984).
- ¹⁸J. L. Cardy, Nucl. Phys. B **240**, 514 (1984).
- ¹⁹F. C. Alcaraz, M. N. Barber, and M. T. Batchelor, Phys. Rev. Lett. **58**, 771 (1987).
- ²⁰F. C. Alcaraz, M. Barber, and M. Batchelor, Ann. Phys. **182**, 280 (1988).
- ²¹S. Eggert, in *Theoretical Survey of One Dimensional Wire Systems*, edited by Y. Kuk *et al.* (Sowha Publishing, Seoul, 2007).
- ²²L. Faddeev and L. Takhtajan, Phys. Lett. A **85**, 375 (1981).
- ²³M. Batchelor, M. Bortz, X.-W. Guan, and N. Oelkers, J. Phys.: Conf. Ser. **42**, 5 (2006).
- ²⁴D. Biegel, M. Karbach, G. Müller, and K. Wiele, Phys. Rev. B **69**, 174404 (2004).
- ²⁵S. Eggert and I. Affleck, Phys. Rev. B **46**, 10866 (1992).
- ²⁶S. Lukyanov and V. Terras, Nucl. Phys. B **654**, 323 (2003).
- ²⁷J. Sirker and M. Bortz, J. Stat. Mech.: Theory Exp. (2006) P01007.
- ²⁸T. Deguchi, K. Fabricius, and B. M. McCoy, J. Stat. Phys. **102**, 701 (2001).
- ²⁹D. Braak and N. Andrei, J. Stat. Phys. **105**, 677 (2001).
- ³⁰K. Fabricius and B. M. McCoy, J. Stat. Phys. **103**, 647 (2001).
- ³¹K. Fabricius and B. M. McCoy, J. Stat. Phys. **104**, 573 (2001).
- ³²K. Nomura, Phys. Rev. B **48**, 16814 (1993).
- ³³F. D. M. Haldane, Phys. Rev. Lett. **67**, 937 (1991).
- ³⁴M. Arikawa, M. Karbach, G. Müller, and K. Wiele, J. Phys. A **39**, 10623 (2006).
- ³⁵M. Karbach and G. Müller, Phys. Rev. B **62**, 14871 (2000).
- ³⁶M. Bortz and J. Stolze, Phys. Rev. B **76**, 014304 (2007).
- ³⁷A. Faribault, P. Calabrese, and J.-S. Caux, J. Stat. Mech.: Theory Exp. (2009) P03018 .
- ³⁸N. Kitanine, K. Kozłowski, J. Maillet, N. Slavnov, and V. Terras, arXiv:0903.2916 (unpublished).
- ³⁹R. Hagemann and J.-S. Caux, J. Phys. A **40**, 14605 (2007).